

# Fine scale thermal blooming instability: a linear stability analysis

John J. Barnard

The fine-scale thermal blooming instability of a high power *trans*-atmospheric laser beam is shown to be affected by the laser pulse length. In this study, we calculate the asymptotic gain of a sinusoidal perturbation as a function of pulse length and perturbation wavenumber. We include the effects of viscosity, diffusion, and wind shear, and we heuristically estimate the effect of turbulence. We find that for short laser pulses, the small wavenumber perturbations are reduced due to acoustic effects. However, large wavenumber perturbations remain large and extend to a higher cutoff in wavenumber than in the long laser pulse limit. At wavenumbers higher than this cutoff, thermal diffusion causes exponential decay of the perturbations. For long laser pulse length wind shear and turbulence limit perturbation growth.

## I. Introduction

It has been known for some time that intense laser beam propagation through the atmosphere results in heating of the atmosphere in the path of the beam. This lowers the air density and index of refraction, which broadens the optical beam in the crosswind direction. This behavior has been termed thermal blooming (see Ref. 1 and references therein for a review). Recent computational<sup>2,3</sup> and theoretical analyses<sup>4-10</sup> show that at high spatial frequencies an instability can develop which is related to thermal blooming of the whole beam and which can (possibly severely) degrade the optical quality of the beam. In Refs. 6 and 7 the authors investigated the damping of the instability in the presence of wind shear. In Refs. 4-8 the instability has been analyzed for two types of laser beam propagation: (1) freely propagating (i.e., uncompensated) beams and (2) phase compensated beams, in which the initial phase has been adjusted so that the beam is collimated on exit from the atmosphere. These investigations have assumed that the laser pulse lengths have been long compared to the sound-crossing time of the beam (typically  $\sim 10^{-2}$  s).

In this paper, we extend the analysis of the instability in beams which are freely propagating to include acoustic effects (i.e., we relax the isobaric assumption of previous work). The inclusion of acoustic effects

allows for calculation of the instability growth rate for pulse times much shorter than those previously analyzed. We also include viscous and diffusive effects. We include both molecular and turbulent diffusion (the latter of which we treat heuristically by using an effective turbulent diffusion coefficient for small perturbation scales and turbulent wind shear for long scales). In Sec. II, we present the general fluid and wave equations which govern the propagation of a laser beam through the atmosphere. In Sec. III we linearize and solve the equations analytically for propagation through an idealized atmosphere. In Sec. IV, we examine how the growth rates are altered when pulse times are even shorter than the transit time of light through the atmosphere. In Sec. V, we estimate the effects of wind shear and turbulence. Finally, in Sec. VI the growth rates are summarized, and some of the implications for pulsing schemes are discussed.

## II. Fluid and Wave Equations

The equations of mass, momentum, and energy conservation for a fluid are, respectively,<sup>11</sup>

$$\frac{\partial}{\partial t} \rho + \frac{\partial}{\partial x_i} (\rho v_i) = 0, \quad (1)$$

$$\frac{\partial}{\partial t} (\rho v_i) + \frac{\partial}{\partial x_k} (P \delta_{ik} + \rho v_i v_k - \sigma'_{ik}) = 0, \quad (2)$$

$$\frac{\partial}{\partial t} \left( \rho \epsilon + \frac{1}{2} \rho v^2 \right) + \frac{\partial}{\partial x_i} \left[ v_i \left( \frac{1}{2} \rho v^2 + \rho \epsilon + P - \sigma'_{ih} \right) - \kappa_T \frac{\partial T}{\partial x_i} \right] = \kappa_A \rho I. \quad (3)$$

Here  $x_i$  and  $v_i$  are the  $i$ th components of the position and velocity vectors of the fluid;  $t$  is time;  $P$ ,  $\rho$ ,  $\epsilon$ , and  $T$

The author is with University of California, Lawrence Livermore National Laboratory, P.O. Box 808, Livermore, California 94550.

Received 2 May 1988.

0003-6935/89/030437-09\$02.00/0.

© 1989 Optical Society of America.

are the pressure, mass density, internal energy per unit mass; and temperature, respectively, of the fluid;  $I$  is the local intensity of the laser beam; and  $\kappa_A$  is the opacity of the fluid so that the laser energy per unit volume absorbed by the fluid in unit time is given by the right-hand side of Eq. (3).  $\kappa_T$  is the thermal conductivity of the fluid, and  $\sigma_{ih}$  is the viscous stress tensor given by<sup>11</sup>

$$\sigma_{ih} = \eta \left( \frac{\partial v_i}{\partial x_h} + \frac{\partial v_h}{\partial x_i} - \frac{2}{3} \delta_{ih} \frac{\partial v_l}{\partial x_l} \right) + \zeta \delta_{ih} \frac{\partial v_l}{\partial x_l}. \quad (4)$$

Here  $\eta$  is the viscosity coefficient, and  $\zeta$  is the second viscosity coefficient. The momentum and energy equations can be written in slightly more convenient forms for the velocity and temperature:

$$\frac{\partial v_i}{\partial t} + v_h \frac{\partial v_i}{\partial x_h} = -\frac{1}{\rho} \frac{\partial P}{\partial x_i} + \frac{\eta}{\rho} \frac{\partial^2 v_i}{\partial x_h \partial x_h} + \left( \zeta + \frac{1}{3} \eta \right) \frac{\partial}{\partial x_i} \left( \frac{\partial v_l}{\partial x_l} \right), \quad (5)$$

$$\begin{aligned} \frac{\partial T}{\partial t} + v_i \frac{\partial T}{\partial x_i} + (\gamma - 1) T \frac{\partial}{\partial x_i} v_i &= \Gamma_T I + \chi \chi \frac{\partial^2 T}{\partial x_h \partial x_h} \\ &+ \frac{(\gamma - 1) \mu m_H}{k_B} \left[ \frac{1}{2} \eta \left( \frac{\partial v_i}{\partial x_h} + \frac{\partial v_h}{\partial x_i} - \frac{2}{3} \delta_{ih} \frac{\partial v_l}{\partial x_l} \right)^2 + \zeta \left( \frac{\partial v_l}{\partial x_l} \right)^2 \right]. \end{aligned} \quad (6)$$

Here  $\gamma$  is the ratio of specific heats,  $\chi$  is the thermometric conductivity [ $\chi = \kappa_T(\gamma - 1) \mu m_H / \gamma k_B \rho$ ], and  $\Gamma_T = \kappa_A(\gamma - 1) \mu m_H / k_B$ . Also, in Eq. (6) we have assumed and made use of the perfect gas law:

$$P = (\gamma - 1) \rho \epsilon = \rho k_B T / (\mu m_H) = \rho c_s^2 / \gamma. \quad (7)$$

Here (and above)  $\mu$ ,  $m_H$ , and  $k_B$  are the mean molecular weight, mass of the hydrogen atom, and Boltzmann's constant, respectively, and  $c_s$  is the sound speed.

The fluid alters the intensity, described via the wave equation

$$\nabla^2 \mathbf{E} = \frac{1}{c^2} \frac{\partial^2 \epsilon \mathbf{E}}{\partial t^2} + \nabla (\mathbf{E} \cdot \nabla \ln \epsilon) = 0. \quad (8)$$

Here  $\mathbf{E}$  is the electric field,  $\epsilon$  is the dielectric constant, and  $c$  is the speed of light in vacuum. We assume a form for  $\mathbf{E}$  in which a light wave propagates in the  $z$  direction with slowly varying amplitude. We define the  $x$ -component of  $\mathbf{E}$  to be

$$\mathbf{E}_x = E_x(x, y, z, t) \exp[i(kz - \omega t)] \hat{\mathbf{e}}_x. \quad (9)$$

Assuming  $\partial/\partial z \ll k$ , and  $\partial/\partial t \ll \omega$ , the paraxial wave equation is obtained:

$$0 = \left[ \frac{\omega^2 \epsilon}{c^2} - k^2 \right] E_x + \nabla_{\perp}^2 E_x + 2i \left[ k \frac{\partial E_x}{\partial z} + \frac{\omega}{c^2} \frac{\partial \epsilon}{\partial t} E_x + \frac{\omega}{c^2} \epsilon \frac{\partial E_x}{\partial t} \right]. \quad (10)$$

We have neglected the third term in Eq. (8), which is appropriate when  $|\nabla_{\perp}| \ll k$ . Here  $\nabla_{\perp}$  is the gradient operating in the plane perpendicular to the propagation direction, which is assumed to be parallel to the  $z$  axis.

### III. Solutions of the Linearized Equations

Following Refs. 4-8 we perform a linear stability analysis of the fluid and wave equations. As in Ref. 4

we express the electric field amplitude in terms of the intensity  $I$  and phase  $S$ :

$$E_x \sim I^{1/2} \exp(ikS). \quad (11)$$

We assume that the equilibrium solution of the wave equation has a spatially and temporally constant intensity  $I_0$  and phase  $S_0$ . We are interested in the evolution of linear perturbations  $I_1$  and  $S_1$ , which in general will be functions of time and space. By substituting Eq. (11) into Eq. (10) and maintaining only linear terms, we obtain

$$\frac{\partial S_1}{\partial z} - \frac{n_1}{n_0} - \frac{1}{4k^2 I_0} \nabla_{\perp}^2 I_1 = -\frac{n_0}{c} \frac{\partial S_1}{\partial t}, \quad (12)$$

$$\frac{\partial I_1}{\partial z} + I_0 \nabla_{\perp}^2 S_1 = -\frac{n_0}{c} \frac{\partial I_1}{\partial t} - \frac{4I_0}{c} \frac{\partial n_1}{\partial t}. \quad (13)$$

Here  $n_1$  is the perturbation in the index of refraction ( $n = \sqrt{\epsilon}$ ), which is assumed to be a function of density only (i.e.,  $n_1 = \rho_1 dn/d\rho$ ).

When pulse lengths are long compared to the light transit time through the atmosphere ( $\sim 10^{-5}$  s), the terms on the right-side of Eqs. (12) and (13) are negligible compared with those on the left. We shall return to Eqs. (12) and (13) in Sec. IV when we consider pulse lengths shorter than light transit times. For longer times these reduce to the phase and intensity equations of Ref. 4:

$$\frac{\partial S_1}{\partial z} = \frac{n_1}{n_0} + \frac{1}{4k^2 I_0} \nabla_{\perp}^2 I_1, \quad (14)$$

$$\frac{\partial I_1}{\partial z} = -I_0 \nabla_{\perp}^2 S_1. \quad (15)$$

We assume an equilibrium density  $\rho_0$ , temperature  $T_0$ , and wind velocity  $\mathbf{v}_0$  (as well as  $I_0$  and  $S_0$ ), which are constants in space and time throughout the beam (i.e., we adopt the box beam hypothesis of Ref. 4). The linearized continuity, velocity, and temperature equations then become

$$\frac{\partial \rho_1}{\partial t} + \mathbf{v}_0 \cdot \nabla \rho_1 + \rho_0 \nabla \cdot \mathbf{v}_1 = 0, \quad (16)$$

$$\frac{\partial v_1}{\partial t} + \mathbf{v}_0 \cdot \nabla \mathbf{v}_1 = \frac{-c_s^2}{\gamma T_0} \nabla T_1 - \frac{c_s^2}{\gamma \rho_0} \nabla \rho_1 + \frac{\eta}{\rho_0} \nabla^2 \mathbf{v}_1 + \frac{\left(\zeta + \frac{1}{3}\eta\right)}{\rho_0} \nabla(\nabla \cdot \mathbf{v}_1), \quad (17)$$

$$\frac{\partial T_1}{\partial t} + \mathbf{v}_0 \cdot \nabla T_1 + (\gamma - 1) T_0 \nabla \cdot \mathbf{v}_1 = \Gamma_T T_1 + \gamma \chi \nabla^2 T_1. \quad (18)$$

We assume that the perturbations vary as  $\exp(i\mathbf{k}_\perp \cdot \mathbf{x})$  and perform a Laplace transform in time with the transformed variables  $\tilde{f}_1$  satisfying  $\tilde{f}_1 = \int_0^\infty \exp(-st) f_1(t) dt$ . Equations (14)–(18) then yield

$$(s + i\mathbf{k}_\perp \cdot \mathbf{v}_0) \tilde{\rho}_1 + i\rho_0 \mathbf{k}_\perp \cdot \hat{\mathbf{v}}_{1\perp} + \rho_0 \frac{\partial \tilde{\rho}_{1z}}{\partial z} = \rho_1(t=0; z), \quad (19)$$

$$(s + i\mathbf{k}_\perp \cdot \mathbf{v}_0) \mathbf{v}_{1\perp} + \left[ \nu \left( k_\perp^2 - \frac{\partial^2}{\partial z^2} \right) + \theta k_\perp^2 \right] \hat{\mathbf{v}}_{1\perp} + \frac{ic_s^2}{\gamma} \left( \frac{\tilde{T}_1}{T_0} + \frac{\tilde{\rho}_1}{\rho_0} \right) \mathbf{k}_\perp - i\theta \mathbf{k}_\perp \frac{\partial \tilde{\rho}_{1z}}{\partial z} = \mathbf{v}_{1\perp}(t=0; z), \quad (20)$$

$$(s + i\mathbf{k}_\perp \cdot \mathbf{v}_0) \tilde{\rho}_{1z} + \left[ \nu \left( k_\perp^2 - \frac{\partial^2}{\partial z^2} \right) - \theta \frac{\partial^2}{\partial z^2} \right] \tilde{\rho}_{1z} + \frac{c_s^2}{\gamma} \left[ \frac{1}{T_0} \frac{\partial \tilde{T}_1}{\partial z} + \frac{1}{\rho_0} \frac{\partial \tilde{\rho}_1}{\partial z} \right] + i\theta \mathbf{k}_\perp \cdot \frac{\partial \tilde{\rho}_{1\perp}}{\partial z} = \rho_{1z}(t=0; z), \quad (21)$$

$$(s + i\mathbf{k}_\perp \cdot \mathbf{v}_0) \tilde{T}_1 + i(\gamma - 1) T_0 \mathbf{k}_\perp \cdot \hat{\mathbf{v}}_{1\perp} + (\gamma - 1) T_0 \frac{\partial \tilde{\rho}_{1z}}{\partial z} + \gamma \chi \left( k_\perp^2 - \frac{\partial^2}{\partial z^2} \right) \tilde{T}_1 = \Gamma_T \tilde{T}_1 + T_1(t=0; z), \quad (22)$$

$$\frac{\partial^2 \tilde{f}_1}{\partial z^2} = I_0 k_\perp^2 \tilde{\rho}_1 - \frac{k_\perp^4}{4k^2} \tilde{f}_1. \quad (23)$$

Here  $\nu = \eta/\rho_0$  and  $\theta = (\zeta + \eta/3)/\rho_0$ . Note that the equation for the phase  $S$  has been eliminated by differentiating Eq. (15) by  $z$  and substituting into Eq. (14).

Laplace transforming in  $z$ , where  $\tilde{g}_1 = \int_0^\infty g_1(z) \exp(-\sigma z) dz$ , we find

$$s_0(\tilde{\rho}_1/\rho_0) + i\mathbf{k}_\perp \cdot \hat{\mathbf{v}}_{1\perp} + \sigma \tilde{\rho}_{1z} = C/\rho_0, \quad (24)$$

$$r_1(\tilde{\rho}_{1\perp}/c_s) + i(c_s k_\perp/\gamma)(\tilde{T}_1/T_0 + \tilde{\rho}_1/\rho_0) - i\theta k_\perp \sigma(\tilde{\rho}_{1z}/c_s) = M_\perp/c_s, \quad (25)$$

$$r_2(\tilde{\rho}_{1z}/c_s) + (c_s \sigma/\gamma)(\tilde{T}_1/T_0 + \tilde{\rho}_1/\rho_0) - i\theta k_\perp \sigma(\tilde{\rho}_{1\perp}/c_s) = M_\parallel/c_s, \quad (26)$$

$$t_0(\tilde{T}_1/T_0) + i(\gamma - 1) \mathbf{k}_\perp \cdot \hat{\mathbf{v}}_{1\perp} + (\gamma - 1) \sigma \tilde{\rho}_{1z} = (\Gamma_T/T_0) \tilde{T}_1 + E/T_0, \quad (27)$$

$$(\sigma^2 + k_\perp^4/4k^2) \tilde{f}_1 - I_0 k_\perp^2 \tilde{\rho}_1 = W. \quad (28)$$

Here

$$C = \tilde{\rho}_1(t=0; \sigma) + \rho_0 \tilde{\rho}_{1z}(z=0; \sigma),$$

$$M_\perp = \tilde{\rho}_{1\perp}(t=0; \sigma) - \nu \sigma \tilde{\rho}_{1z}(z=0; \sigma)$$

$$- i\theta k_\perp \tilde{\rho}_{1z}(z=0; \sigma) - \nu \sigma \frac{\partial \tilde{\rho}_{1\perp}}{\partial z}(z=0; \sigma),$$

$$M_\parallel = \rho_{1z}(t=0; \sigma) + (c_s^2/\gamma)$$

$$\times [T_1(z=0; \sigma)/T_0 + \tilde{\rho}_1(z=0; \sigma)/\rho_0]$$

$$- (\nu + \theta) [\sigma \tilde{\rho}_{1z}(z=0; \sigma)$$

$$+ \frac{\partial \tilde{\rho}_{1z}}{\partial z}(z=0; \sigma)] + i\theta k_\perp \tilde{\rho}_{1\perp}(z=0; \sigma),$$

$$E = (\gamma - 1) T_0 \tilde{\rho}_{1z}(z=0; \sigma) - \chi \sigma \tilde{T}_1(z=0; \sigma) - \chi \frac{\partial \tilde{T}_1}{\partial z}(z=0; \sigma),$$

$$W = \sigma \tilde{f}_1(z=0; \sigma) + \frac{\partial \tilde{f}_1}{\partial z}(z=0; \sigma).$$

Also,  $s_0 = s + i\mathbf{k}_\perp \cdot \mathbf{v}_0$ ,  $t_0 = s_0 + \gamma \chi (k_\perp^2 - \sigma^2)$ ,  $r_0 = s_0 + \nu (k_\perp^2 - \sigma^2)$ ,  $r_1 = r_0 + \theta k_\perp^2$ ,  $r_2 = r_0 - \theta \sigma^2$ ,  $p_0 = s_0 + (\nu + \theta)(k_\perp^2 - \sigma^2)$ ,  $\mathbf{v}_\perp = (\mathbf{k}_\perp \cdot \mathbf{v}_{1\perp})/\mathbf{k}_\perp$ ,  $k_\perp = |\mathbf{k}_\perp|$ .

The fluid equations [Eqs. (24)–(27)] may be expressed as a matrix equation

$$\mathbf{M}\mathbf{v} = \mathbf{C}_0 + (\Gamma_T/T_0) \tilde{f}_1 \hat{\mathbf{e}}_4, \quad (29)$$

where

$$\mathbf{M} \equiv \begin{bmatrix} s_0 & \sigma c_s & ic_s k_\perp & 0 \\ ic_s k_\perp/\gamma & q & r_1 & ic_s k_\perp/\gamma \\ c_s \sigma/\gamma & r_2 & q & c_s \sigma/\gamma \\ 0 & (\gamma - 1) c_s \sigma & i(\gamma - 1) c_s k_\perp & t_0 \end{bmatrix}, \quad (30)$$

$$\mathbf{v} = \begin{bmatrix} \tilde{\rho}_1/\rho_0 \\ \tilde{\rho}_{1z}/c_s \\ \tilde{\rho}_{1\perp}/c_s \\ \tilde{T}_1/T_0 \end{bmatrix}; \quad \mathbf{C}_0 = \begin{bmatrix} C/\rho_0 \\ M_\parallel/c_s \\ M_\perp/c_s \\ E/T_0 \end{bmatrix}; \quad \hat{\mathbf{e}}_4 = \begin{bmatrix} 0 \\ 0 \\ 0 \\ 1 \end{bmatrix}. \quad (31)$$

Here  $q = -i\theta k_\perp \sigma$ . Solving Eq. (29) for  $\mathbf{v}$  yields

$$\mathbf{v} = \mathbf{M}^{-1} \mathbf{C}_0 + \mathbf{M}^{-1} \hat{\mathbf{e}}_4 \left( \frac{\Gamma_T}{T_0} \tilde{f}_1 \right), \quad (32)$$

The first component of Eq. (32) is

$$\tilde{\rho}_1/\rho_0 = (M^{-1})_{11}C_{01} + (M^{-1})_{14}(\Gamma_T \tilde{T}_1/T_0). \quad (33)$$

The perturbation to the index of refraction is thus

$$\tilde{n}_1 = (dn/d\rho)\rho_0(M^{-1})_{11}C_{01} + (dn/d\rho)(\rho_0\Gamma_T/T_0)(M^{-1})_{14}\tilde{T}_1. \quad (34)$$

Substitution of Eq. (34) into the transformed wave equation, Eq. (28), yields

$$\begin{aligned} [\sigma^2 + k_{\perp}^4/4k^2 - I_0k_{\perp}^2(dn/d\rho)(\rho_0\Gamma_T/T_0)(M^{-1})_{14}]\tilde{T}_1 \\ = W + I_0k_{\perp}^2\rho_0(dn/d\rho)(M^{-1})_{11}C_{01}. \end{aligned} \quad (35)$$

We let  $\Gamma = (1/\gamma)(dn/d\rho)(\rho_0/T_0)\Gamma_T$  and define

$$B_0 = W + I_0k_{\perp}^2\rho_0(dn/d\rho)(M^{-1})_{11}C_{01}. \quad (36)$$

Equation (35) can be written

$$\tilde{T}_1 = \frac{B_0}{\sigma^2 + \frac{k_{\perp}^4}{4k^2} + \frac{\Gamma I_0k_{\perp}^2[k_{\perp}^2 - \sigma^2]}{s_0t_0\rho_0/c_s^2 + (k_{\perp}^2 - \sigma^2)[(\gamma-1)s_0 + t_0]/\gamma}}. \quad (37)$$

Here we have made use of

$$\det(M) = -s_0t_0\rho_0 + c_s^2(\sigma^2 - k_{\perp}^2)r_0[(\gamma-1)s_0 + t_0]/\gamma, \quad (38)$$

$$(M^{-1})_{14} = \frac{\text{cof}(M_{41})}{\det(M)} = \frac{c_s^2r_0(k_{\perp}^2 - \sigma^2)/\gamma}{\det(M)}. \quad (39)$$

The Laplace inversion of Eq. (37) yields

$$I_1(z,t) = \frac{-1}{4\pi^2} \int_{c_1-i\infty}^{c_1+i\infty} \int_{c_2-i\infty}^{c_2+i\infty} \frac{ds ds' \exp(st + \sigma z) B_0}{D(\sigma, s)}, \quad (40)$$

where

$$\begin{aligned} D(\sigma, s) = \sigma^2 + \frac{k_{\perp}^4}{4k^2} \\ + \frac{\Gamma I_0k_{\perp}^2(k_{\perp}^2 - \sigma^2)}{s_0t_0\rho_0/c_s^2 + (k_{\perp}^2 - \sigma^2)[(\gamma-1)s_0 + t_0]/\gamma}. \end{aligned} \quad (41)$$

We assume that variations in  $z$  are much slower than variations in  $x$  and  $y$ :

$$|\sigma^2| \ll k_{\perp}^2. \quad (42)$$

Physically, Eq (42) is equivalent to the assumption that the growth length and the perturbation Rayleigh length ( $\sim 2k/k_{\perp}^2$ ) are both much larger than the wavelength of the perturbation ( $2\pi/k_{\perp}$ ). The smallest relevant  $k_{\perp}$  is of the order of  $2\pi/a$ , where  $a$  is the laser beam diameter. The spatial growth length is  $\sim z/G$ , where  $G$  is the logarithmic gain of the perturbation [Eq. (50)]. Equation (42) is easily satisfied (*a posteriori*) for the parameters used in Fig. 1.

$D(\sigma, s)$  has a zero, and hence the integrand of Eq. (40) has a pole when

$$\begin{aligned} \sigma \approx \pm i \left\{ \frac{k_{\perp}^4}{4k^2} \right. \\ \left. + \frac{\Gamma I_0k_{\perp}^4}{s_0(s_0 + \gamma\chi k_{\perp}^2)[s_0 + (\nu + \theta)k_{\perp}^2]/c_s^2 + k_{\perp}^2(s_0 + \chi k_{\perp}^2)} \right\}^{1/2}. \end{aligned} \quad (43)$$

Evaluating the residue implies that

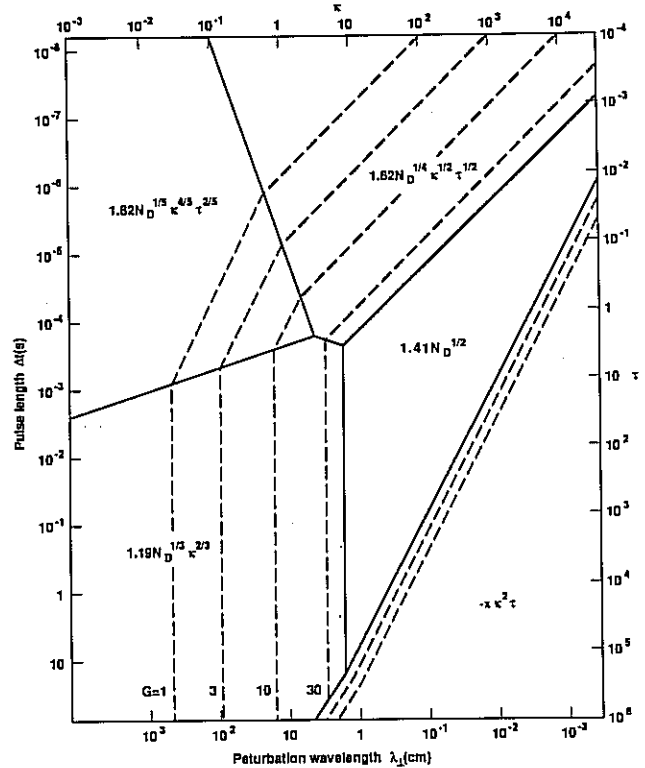


Fig. 1. Schematic representation of thermal blooming gain in the  $\kappa - \tau$  plane. Asymptotic regimes and the respective gains for each region are shown. Dashed lines indicate contours of constant gain. The four contours shown are for  $G = 1, 3, 10$ , and  $30$ . Double dashed lines schematically indicate closely spaced contours lines due to the decay of the perturbations from thermal diffusion. The distortion number,  $N_D = \Gamma I_0 k z t$ , is held constant. The normalized variables are  $\kappa = (z/2k)^{1/2} k_{\perp}$ ,  $\tau = (2k/z)^{1/2} c_s t$ ,  $x = (2k/z)^{1/2} \chi/c_s$ , and  $\lambda_{\perp} = 2\pi/k_{\perp}$ . For this figure the following parameters have been assumed:  $N_D = 1000$ ,  $z = 5 \times 10^5$  cm,  $k = 6.3 \times 10^4$  cm $^{-1}$ ,  $\chi = 0.22$  cm $^2$ s $^{-1}$ ,  $v_0 = 0$ ,  $c_s = 3 \times 10^4$  cm s $^{-1}$ .

$$I_1(z,t) \sim \exp(-ik_{\perp} \cdot \mathbf{v}_0 t) \int_{c_2-i\infty}^{c_2+i\infty} ds_0 g(s_0) \exp(\varphi), \quad (44)$$

where

$$\varphi \equiv \sigma(s_0)z + s_0 t. \quad (45)$$

When  $|\varphi| \gg 1$ , the integral may be evaluated by the method of steepest descents. In that case the behavior for large  $z$  and  $t$  is given by

$$I_1(z,t) \sim \sum_i \exp[\varphi(s_{0i})], \quad (46a)$$

where

$$\frac{d\varphi}{ds_0} = 0 \text{ at } s_0 = s_{0i}. \quad (46b)$$

In Eq. (46a) the summation is over all roots  $s_{0i}$  that satisfy Eq. (46b). Using Eqs. (43) and (45) we obtain

$$\frac{d\varphi}{ds_0} = \frac{3\Gamma I_0 k_{\perp}^4 z}{2\sigma c_s^2} \frac{[s_0^2 + \frac{2}{3}(\gamma\chi + \nu + \theta)k_{\perp}^2 s_0 + \frac{1}{3}c_s^2 k_{\perp}^2]}{[s_0(s_0 + \gamma\chi k_{\perp}^2)(s_0 + (\nu + \theta)k_{\perp}^2/c_s^2 + k_{\perp}^2(s_0 + \chi k_{\perp}^2))]^2} + t. \quad (47)$$

For long times  $c_s k_{\perp} \gg |s_0|$  and  $c_s^2/\chi \gg |s_0|$ ,

$$0 = \frac{\pm i\Gamma I_0 z}{[k_{\perp}^4/4k^2 + \Gamma I_0 k_{\perp}^2/(s_0 + \chi k_{\perp}^2)]^{1/2}(s_0 + \chi k_{\perp}^2)} + t. \quad (48)$$

Physically, the assumption  $c_s k_{\perp} \gg |s_0|$  corresponds to a sound transit time of the perturbation  $\tau_s$  that is short compared with the growth time of the perturbation  $\tau_G = t/G$ . The assumption  $c_s^2/\chi \gg |s_0|$  corresponds to  $\tau_s \ll (\tau_G \tau_D)^{1/2}$ , where  $\tau_D = 1/\chi k_{\perp}^2$  is the diffusion time. For the parameters in Fig. 1, if the first condition is met, the second condition is automatically satisfied since  $\tau_D \gg \tau_s$  over the range of  $k_{\perp}$  in the diagram.

This equation has the approximate solutions

$$s_0 \approx \begin{cases} (\pm i)^{1/2} (\Gamma I_0 k z / t)^{1/2} - \chi k_{\perp}^2 & \text{if } |s_0 + \chi k_{\perp}^2| \gg \frac{4k^2 \Gamma I_0}{k_{\perp}^2}, \\ \left(\frac{\pm i}{2}\right)^{1/2} (\Gamma I_0 k_{\perp}^2 z^2 / t^2)^{1/3} - \chi k_{\perp}^2 & \text{if } |s_0 + \chi k_{\perp}^2| \ll \frac{4k^2 \Gamma I_0}{k_{\perp}^2}. \end{cases} \quad (49)$$

The total logarithmic gain  $G = \text{Re}(\varphi)$  can thus be approximately written

$$G \approx \begin{cases} 1.2(N_D \kappa^2)^{1/3} & \text{if } \kappa \ll N_D^{1/4}, \kappa \gg N_D/\tau^3, \\ 1.4N_D^{1/2} & \text{if } \kappa \gg N_D^{1/4}, \kappa \gg N_D^{1/2}/\tau, \\ -x\kappa^2\tau & \text{if } N_D \gg G \text{ (as defined above)}. \end{cases} \quad (50)$$

Here  $N_D = \Gamma I_0 k z t$ ,  $N_{\chi} = \chi k_{\perp}^2 t = x\kappa^2\tau$ ,  $\kappa = (z/2k)^{1/2} k_{\perp}$ ,  $\tau = (2k/z)^{1/2} c_s t$ , and  $x = (2k/z)^{1/2} \chi/c_s$ .

In Eq. (50), the maximum gain occurs when  $t = \Delta t$  (the laser pulse length) and  $z = h$  (the height of the atmosphere). These same results were found in Ref. 4, except for the presence of the diffusion term in Eq. (50).

We now turn our attention to short pulse lengths in which  $c_s k_{\perp} \ll |s_0|$  (but still long compared to a light transit time through the atmosphere). In this limit Eq. (47) can be written

$$1 \approx \pm \frac{3}{2} i \left( \frac{\Gamma I_0 k_{\perp}^4 c_s^2 z}{s_0 t} \right) \frac{[s_0 + \frac{2}{3}(\gamma\chi + \nu + \theta)k_{\perp}^2]}{\left\{ \frac{k_{\perp}^4}{4k^2} + \frac{\Gamma I_0 k_{\perp}^4 c_s^2}{s_0(s_0 + \gamma\chi k_{\perp}^2)(s_0 + (\nu + \theta)k_{\perp}^2)} \right\}^{1/2} (s_0 + \gamma\chi k_{\perp}^2)^2 [s_0 + (\nu + \theta)k_{\perp}^2]^2} \quad (51)$$

In the limit  $1/4k^2 \ll |\Gamma I_0 c_s^2/s_0^3|$  the equation can be written

$$1 \approx \frac{s_1^{5/2}(s_0 + s_4)}{s_0^{1/2}(s_0 + s_2)^{3/2}(s_0 + s_3)^{3/2}}, \quad (52)$$

where  $s_1^{5/2} = \pm i(3z/2c_s t)(\Gamma I_0)^{1/2}(c_s k_{\perp})^2$ ,  $s_2 = \gamma\chi k_{\perp}^2$ ,  $s_3 = (\nu + \theta)k_{\perp}^2$ ,  $s_4 = \frac{2}{3}(\gamma\chi + \nu + \theta)k_{\perp}^2$ . If  $|s_1| \gg |s_2|, |s_3|, |s_4|$ , the dominant contribution to the saddle point integral occurs when  $s_0 \approx s_1$ . If  $|s_1| \ll |s_2|, |s_3|, |s_4|$ , saddle points occur when  $s_0 \approx -s_2$  and  $s_0 \approx -s_3$ , corresponding to decay modes caused primarily by viscosity [ $s_0 \approx -(\nu + \theta)k_{\perp}^2$ ] or thermal diffusion [ $s_0 \approx -\gamma\chi k_{\perp}^2$ ]. For air these decay rates are comparable.

In the limit when diffraction is important,  $1/4k^2 \gg |\Gamma I_0 c_s^2/s_0^3|$ ; then Eq. (51) can be written

$$1 = \frac{s_5^4(s_0 + s_4)}{s_0(s_0 + s_2)^2(s_0 + s_3)^2}, \quad (53)$$

where  $s_5^4 = \pm i 3 \Gamma I_0 c_s^2 k_{\perp}^2 k z / t$ . If  $|s_5| \gg |s_2|, |s_3|, |s_4|$  the dominant saddle point occurs at  $s_0 \approx s_5$ . When  $|s_5| \ll |s_2|, |s_3|, |s_4|$ , the thermal and viscous decay modes dominate as before.

The total logarithmic gain is again found by insertion of the saddle point into Eq. (45) and taking the real part of  $\varphi$ :

$$G \sim \begin{cases} 1.8(N_D \kappa^4 \tau^2)^{1/6} & \text{if } \kappa \ll N_D^{1/6} \tau^{1/3}, \kappa \ll N_D/\tau^3, \\ 1.6(N_D \kappa^2 \tau^2)^{1/4} & \text{if } \kappa \gg N_D^{1/6} \tau^{1/3}, \kappa \ll N_D^{1/2}/\tau, \\ -\max(\gamma N_{\chi}, N_{\nu}) & \text{if } N_{\chi}, N_{\nu} \gg G \text{ (above)}. \end{cases} \quad (54)$$

Here  $N_{\nu} = (\nu + \theta)k_{\perp}^2 t$ .

Equations (50) and (54) give the gain for the thermal blooming instability for various parameters. It is of interest to investigate how the logarithmic gain  $G$  varies when the wavenumber  $k_{\perp}$  and pulse time  $\Delta t$  are varied, and the quantity  $I_0 \Delta t$  (or equivalently  $N_D$ ) is held constant. Figure 1 delimits the various asymptotic regimes (in the  $k_{\perp}, \Delta t$  plane) with the asymptotic gain labeled for each region and a few approximate contours given. The asymptotic formulas should be valid when a point in the  $k_{\perp}, \Delta t$  plane lies far from an asymptotic boundary.

#### IV. Very Short Pulse Times

When the pulse time is shorter than the propagation time through the atmosphere, Eqs. (12) and (13) must be used rather than Eqs. (14) and (15). In that case Eq. (28) becomes

$$\left\{ \left( \sigma + \frac{n_0}{c} s \right)^2 + \frac{k_{\perp}^4}{4k^2} \right\} \tilde{I}_1 - I_0 \left[ \frac{k_{\perp}^2}{n_0} - \frac{4}{c} \left( \sigma + \frac{n_0}{c} s \right) \right] \tilde{n}_1 = W'. \quad (55)$$

Here  $W'$  depends on initial and boundary conditions, the exact form of which is not needed for this discussion. We assume as before that  $|\sigma| \ll k_{\perp}$  and also that  $|s/c| \ll k_{\perp}$ . As long as growth times are substantially longer than light transit times across a perturbation, the latter approximation is valid, as it is for the parameters in Fig. 1. In this case, the second term within the square brackets above is negligible compared with the first.

Repeating the steps to Eq. (43) we find

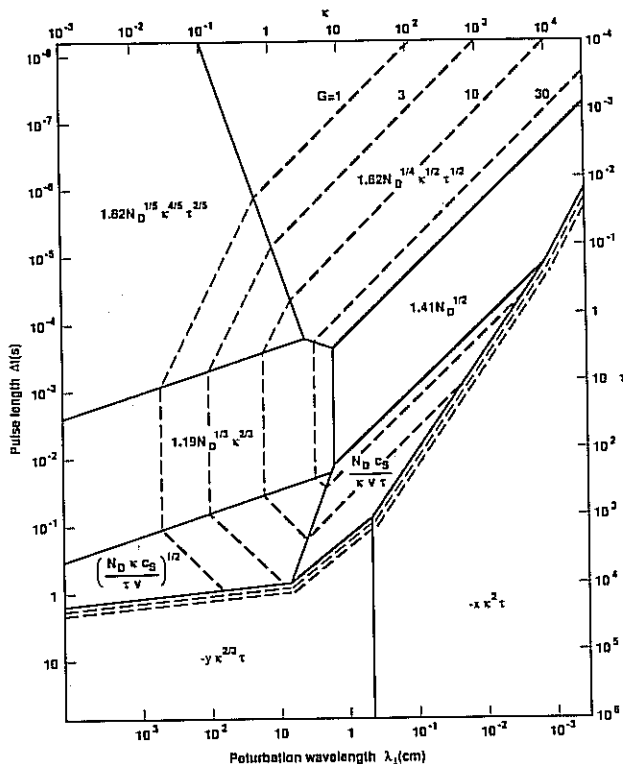


Fig. 2. Schematic representation of thermal blooming gain in the  $\kappa - \tau$  plane. Same as for Fig. 1 except wind shear and the heuristic description of turbulence (described in text) have been included. Double dashed lines indicate the borders of the regions where diffusion (turbulent and molecular) results in decaying perturbations. The variables are the same as in Fig. 1 with the addition that  $y = (z/2k)^{1/6} \epsilon_t^{1/3} / c_s = (z/2k l^2)^{1/6} (v_t/c_s)$ . The parameters are the same as in Fig. 1 except that  $v_0 = 450 \text{ cm s}^{-1}$  and  $\epsilon_t = 180 \text{ cm}^2 \text{ s}^{-1}$ .

$$\sigma = \frac{-n_0 s}{c} + \sigma_0, \quad (56)$$

where  $\sigma_0$  is the solution [Eq. (43)] without inclusion of the light transit time effects.

The saddle point occurs when  $d\varphi/ds = 0$ . Hence

$$0 = t - \frac{n_0}{c} z + \frac{d\sigma_0}{ds} z. \quad (57)$$

Thus the growth rates are identical to those previously obtained on replacement of  $t$  with  $t - n_0 z/c$ . The rates are valid only within the laser pulse, i.e., when  $t$  and  $z$  satisfy  $n_0 z/c \leq t \leq n_0 z/c + \Delta t$ . If the transit time is much shorter than a pulse time this correction is negligible. When the pulse time is much shorter than a transit time, the maximum gain occurs when  $t - n_0 z/c = \Delta t$ . Thus the maximum gain calculated in Secs. III and IV is found using Eqs. (50) and (54) and replacing  $t$  with pulse length  $\Delta t$ .

We should note that for very short pulse times, other physical effects, which have been ignored in this calculation, can become important. In particular, we estimate that for  $\Delta t \lesssim 10^{-6} \text{ s}$  (for parameters of Fig. 1) electrostriction and nonlinear index of refraction effects (Kerr effect) will alter the growth rate. Also, at very short pulse times, coupling of the perturbations to spatial and temporal gradients of the equilibrium in-

tensity can substantially affect growth of the instability.

## V. Wind Shear and Turbulence

The actual atmosphere does not have a velocity profile in which the wind velocity is a constant. Both large-scale shear and fluctuating random components (turbulence) can be present (see, for example, Ref. 12 for experimental measurements). Large-scale shear (both random and systematic) will phase mix and limit the growth of the instability. Small-scale turbulence can convect heat out of a hot spot in a manner analogous to thermal diffusion. We shall nonrigorously estimate the magnitude of both effects.

Theories of turbulence<sup>12-15</sup> and experiments suggest that often a Kolmogorov spectrum may describe the atmosphere. In this theory, energy is deposited into the atmosphere at a rate  $\epsilon_t$  per unit mass, per unit volume, per unit time, on the scale  $l$  of the largest eddies. If  $u$  is the speed of the largest eddy,

$$\epsilon_t \sim u^3/l. \quad (58)$$

On scales  $\lambda$  smaller than  $l$ , it is assumed that the speed associated with that scale can depend only on  $\epsilon_t$  and  $\lambda$ . Hence, on dimensional grounds,

$$v(\lambda) \sim \epsilon_t^{1/3} \lambda^{1/3}. \quad (59)$$

The effective turbulent diffusion coefficient is then obtained:

$$\chi_{\text{turb}}(\lambda) \sim v(\lambda) \lambda \sim \epsilon_t^{1/3} \lambda^{4/3} \sim (2\pi)^{4/3} \epsilon_t^{1/3} k_{\perp}^{-4/3}. \quad (60)$$

Here the final approximate equality sign associates eddy size  $\lambda$  with perturbation wavelength  $2\pi/k_{\perp}$ .

Equation (60) may be used for scale lengths such that  $\lambda_0 \ll \lambda \ll l$ , where  $\lambda_0 = \chi^{3/4}/\epsilon_t^{1/4}$  and where  $\chi$  is the thermal conductivity defined as in Eq. (6). Equation (60) can be used in Eqs. (50) and (54) to estimate the effect that turbulent heat transfer on small scales has on thermal blooming. The regimes (large times and large perturbation wavelengths) where this effect is important are plotted in Fig. 2.

To estimate heuristically the effect of large-scale phase mixing by turbulent or systematic wind shear, we return to Eq. (23):

$$\frac{\partial^2 \tilde{I}_1}{\partial z^2} + \frac{k_{\perp}^4}{4k^3} \tilde{I}_1 = I_0 k_{\perp}^2 \tilde{A}_1 \quad (61)$$

and the equivalent of Eqs. (18), (33), and (34) in the isobaric approximation (long-time limit)<sup>4</sup>:

$$\frac{\partial n_1}{\partial t} + \mathbf{v} \cdot \nabla n_1 = -\Gamma I_1. \quad (62)$$

As will be shown, wind shear will alter the growth rate for perturbations in which the wind shear time,  $1/k_{\perp} v'$ , is shorter than the growth time  $t/G$ , where  $v' = dv/dz$  is the wind velocity gradient. Since acoustic effects become important when  $t/G \ll 1/c_s k_{\perp}$ , and since  $c_s \gg v$ , the isobaric approximation should normally be sufficient when including wind shear effects. Laplace transforming Eq. (62) in time and assuming that quantities vary as  $\exp(ik_{\perp} \cdot \mathbf{x})$  yield

$$\frac{\partial^2 I_1}{\partial z^2} + \left[ \frac{k_{\perp}^4}{4k^2} + \frac{\Gamma I_0 k_{\perp}^2}{s + i\mathbf{k}_{\perp} \cdot \mathbf{v}(z)} \right] I_1 = \frac{I_0 k_{\perp}^2 n_1(t=0; z)}{s + i\mathbf{k}_{\perp} \cdot \mathbf{v}(z)}. \quad (63)$$

Equation (63) assumes that the velocity vector lies in the  $x$ - $y$  plane and is a function only of  $z$ .

The form of Eq. (63) suggests<sup>16</sup> that the WKB method be used to solve it:

$$I_1(z, s) \cong \left[ \frac{k_{z0}}{k_z(z)} \right]^{1/2} \left\{ I_{\pm} \exp \left[ \pm i \int_0^z k_z(z') dz' \right] \right\} + p(z). \quad (64)$$

Here  $I_{\pm}$  are coefficients for the two linearly independent solutions of the homogeneous Eq. (63) that satisfy the boundary conditions on  $I_1(z=0)$  and  $\partial I_1/\partial z(z=0)$ . The function  $p(z)$  is the particular solution, which depends on the initial index of refraction perturbation is the particular solution, which depends on the initial index of refraction perturbation spectrum:

$$p(z) = \frac{I_0 k_{\perp}^2}{k_z^{1/2}(z)} \int_0^z \frac{n_1(t=0; z')}{[s + i\mathbf{k}_{\perp} \cdot \mathbf{v}(z')] k_z^{1/2}(z')} \times \left[ \sin \int_{z'}^z k_z(z'') dz'' \right] dz'.$$

Here  $k_z^2 = k_{\perp}^4/4k^2 + \Gamma I_0 k_{\perp}^2/[s + i\mathbf{k}_{\perp} \cdot \mathbf{v}(z)]$ , and  $k_{z0} = k_z(z=0)$ .

Inverting the Laplace transform, we obtain

$$I_1(z, t) = \frac{I_{\pm}}{2\pi i} \int_{c-i\infty}^{c+i\infty} \left[ \frac{k_{z0}}{k_z(z)} \right]^{1/2} \times \exp \left[ st \pm i \int_0^z k_z(z', s) dz' \right] ds + P(z, t).$$

Here  $P(z, t)$  is the part of the solution due to the particular solution in Eq. (64).

The argument of the exponential in the WKB solution is

$$\varphi = st \pm i \int_0^z k_z(z', s) dz'. \quad (65)$$

Thus the equation for the saddlepoint becomes

$$0 = t \pm i \int_0^z \frac{dk_z(z', s)}{ds} dz'. \quad (66)$$

Solving Eq. (66) for  $s$  and inserting the result into Eq. (65) yield the asymptotic argument of the exponential. The WKB solution obtained in this manner will be valid provided that  $|(1/k_z)(dk_z/dz)| \ll |k_z|$ ; i.e., the change in  $k_z$  in one wavelength ( $2\pi/k_z$ ) is much less than  $|k_z|$ .

As before we search for the gain in asymptotic regimes:

$$\frac{dk_z}{ds} \cong \begin{cases} \frac{-\Gamma I_0 k}{(s + i\mathbf{k}_{\perp} \cdot \mathbf{v})^2} & \frac{k_{\perp}^4}{4k^2} \gg \left| \frac{\Gamma I_0 k_{\perp}^2}{s + i\mathbf{k}_{\perp} \cdot \mathbf{v}} \right|, \\ \frac{(-\Gamma I_0)^{1/2} k_{\perp}}{2(s + i\mathbf{k}_{\perp} \cdot \mathbf{v})^{3/2}} & \frac{k_{\perp}^4}{4k^2} \ll \left| \frac{\Gamma I_0 k_{\perp}^2}{s + i\mathbf{k}_{\perp} \cdot \mathbf{v}} \right|, \end{cases} \quad (67)$$

$$k_z \cong \begin{cases} \frac{k_{\perp}^2}{2k} + \frac{\Gamma I_0 k}{s + i\mathbf{k}_{\perp} \cdot \mathbf{v}} & \frac{k_{\perp}^4}{4k^2} \gg \left| \frac{\Gamma I_0 k_{\perp}^2}{s + i\mathbf{k}_{\perp} \cdot \mathbf{v}} \right|, \\ \left( \frac{-\Gamma I_0 k_{\perp}^2}{s + i\mathbf{k}_{\perp} \cdot \mathbf{v}} \right)^{1/2} & \frac{k_{\perp}^4}{4k^2} \ll \left| \frac{\Gamma I_0 k_{\perp}^2}{s + i\mathbf{k}_{\perp} \cdot \mathbf{v}} \right|. \end{cases} \quad (68)$$

To proceed further we need to specify the velocity as a function of  $z$ . For the case of a steady linear systematic wind shear we assume

$$\mathbf{k}_{\perp} \cdot \mathbf{v} = \mathbf{k}_{\perp} \cdot \mathbf{v}_0 + k_{\perp} v' z. \quad (69)$$

Using Eqs. (66)–(69), in the large  $k_{\perp}$  regime saddle points occur at

$$s_0 \cong \begin{cases} \pm i \left( \frac{i\Gamma I_0 k z}{t} \right)^{1/2} & \text{if } k_{\perp} v' z \ll \left( \frac{\Gamma I_0 k z}{t} \right)^{1/2}, \\ \frac{\Gamma I_0 k}{k_{\perp} v' t}, -ik_{\perp} v' z - \frac{\Gamma I_0 k}{k_{\perp} v' t} & \text{if } k_{\perp} v' z \gg \left( \frac{\Gamma I_0 k z}{t} \right)^{1/2}. \end{cases} \quad (70)$$

The resulting gain is thus

$$G \cong \begin{cases} (2\Gamma I_0 k z t)^{1/2} & \text{for } t \ll t_{\text{crit1}}, \\ [1 + \ln(t/t_{\text{crit1}})](\Gamma I_0 k/k_{\perp} v') & \text{for } t \gg t_{\text{crit1}}. \end{cases} \quad (71)$$

Here  $t_{\text{crit1}} = \Gamma I_0 k/(k_{\perp}^2 v'^2 z)$ . The upper part of the equations in Eq. (71) is the now familiar result in Ref. 4, the lower indicating a saturation for times larger than  $\sim t_{\text{crit1}}$ . Physically  $t_{\text{crit1}}$  is simply the critical time found by equating the growth time  $(t/\Gamma I_0 k z)^{1/2}$  to the wind clearing time of the perturbation  $(1/k_{\perp} v' z)$  and solving for the time. The gain is found approximately by inserting  $t_{\text{crit1}}$  into the standard Briggs result [the upper of Eq. (71)]. Thus in the wind-shearing case the logarithmic gain grows at  $t^{1/2}$  until  $t = t_{\text{crit1}}$  at which point it reaches a plateau, henceforth growing only logarithmically.

In the small  $k_{\perp}$  regime the saddle points are given by

$$s_0 \cong \begin{cases} (\pm i)^{2/3} (\Gamma I_0 k_{\perp}^2 z^2/t^2)^{1/3} & \text{for } t \ll t_{\text{crit2}}, \\ \frac{\Gamma I_0}{v'^2 t^2}, -ik_{\perp} v' z \pm (-i)^{1/2} \left( \frac{\Gamma I_0 k_{\perp} z}{v' t^2} \right)^{1/2} & \text{for } t \gg t_{\text{crit2}}. \end{cases} \quad (72)$$

Here  $t_{\text{crit2}} = [\Gamma I_0/(v'^3 k_{\perp} z)]^{1/2}$ .

The gain becomes

$$G \cong \begin{cases} (\Gamma I_0 k_{\perp}^2 z^2 t)^{1/3} & \text{for } t \ll t_{\text{crit2}}, \\ (\Gamma I_0 k_{\perp} z/v')^{1/2} & \text{for } t \gg t_{\text{crit2}}. \end{cases} \quad (73)$$

Note that the lower part of Eq. (73) agrees with that of Ref. 7 [Perkins's Eq. (32)], while the lower part of Eq. (71) can be made to agree with Eq. (20) in Ref. 6, if  $f(v) = v$  in Rosenbluth's notation. Figure 2 shows where these growth rates are pertinent. Here we have used  $k_{\perp} v' z = k_{\perp} v_0$ , where  $v_0 = 450$  cm/s, to illustrate the magnitude of this type of damping. Note also that, with wind shear, diffusion becomes important at shorter times than without wind shear, because wind shear limits the growth of instability but does not lower the diffusive decay rate.

As pointed out by Rosenbluth,<sup>6</sup> when the direction of shear is perpendicular to  $\mathbf{k}_{\perp}$  ( $k_{\perp} v' z = 0$ ), instability growth occurs as though there were no shear. Thus a purely systematic wind profile given by Eq. (69) will be essentially unaffected by shear for directions of  $\mathbf{k}_{\perp}$  so that  $k_{\perp} v' z = 0$ . However, for an atmosphere with a Kolmogorov velocity spectrum, the turbulence in the inertial range is assumed to be isotropic. Thus for all  $\mathbf{k}_{\perp}$ , there is apparently no preferred direction in which the shear will not lower the growth rate. We estimate the effect of turbulent shear by replacing Eq. (69) with

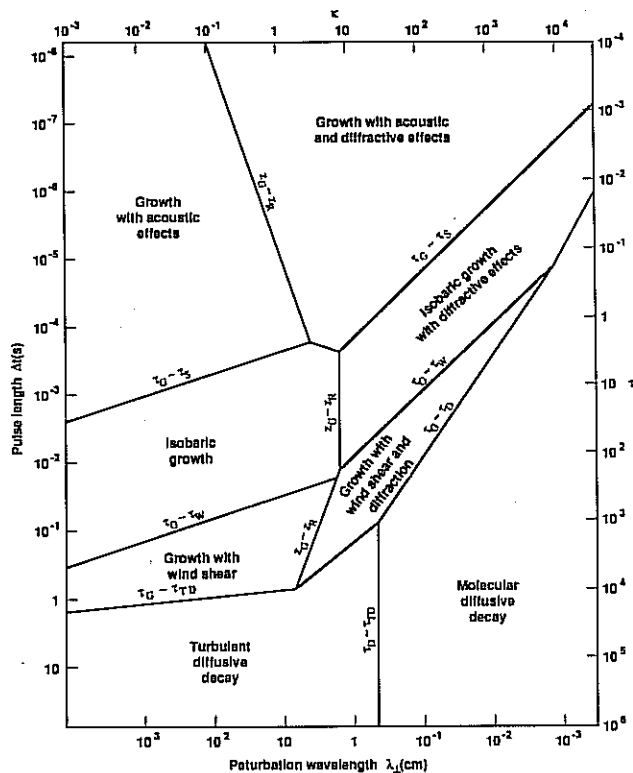


Fig. 3. Physical regimes in the  $k_{\perp} - \tau$  plane. Each regime in Fig. 2 is labeled according to the dominant physical processes. Although the borders between regimes are formally the lines where adjacent asymptotic growth rates are equal, they correspond approximately to the equality of physically meaningful time scales or length scales.  $\tau_G$  = growth time =  $t/G$ ,  $\tau_s$  = perturbation sound crossing time =  $2\pi/(c_s k_{\perp})$ ,  $\tau_W$  = perturbation wind shearing time =  $2\pi/(\nu' z k_{\perp})$ . (We assume  $\nu' z = \nu$ , so  $\tau_W$  is essentially the perturbation wind clearing time as well.)  $\tau_D$  = perturbation molecular diffusion time =  $1/(\chi k_{\perp}^2)$ ,  $\tau_{TD}$  = perturbation turbulent diffusion time =  $1/(\chi_{\text{turb}} k_{\perp}^2) = 1/[(2\pi)^{4/3} \epsilon_t^{1/3} k_{\perp}^{2/3}]$ ,  $z_G$  = growth length =  $z/G$ , and  $z_R$  = perturbation Rayleigh length =  $2k/k_{\perp}^2$ .

$$\dot{v}(z) = v_t(z/l)^{\alpha}. \quad (74)$$

Here, if  $\alpha = 1/3$ , the physics of Eq. (59) should be qualitatively modeled by use of Eq. (74). Repeating the procedure following Eq. (69) we find a saddle point in, for example, the large  $k_{\perp}$  regime at

$$s_0 \approx -ik_{\perp} v_t \left( \frac{z}{l} \right)^{\alpha} \pm \frac{\Gamma I_0 k l}{\alpha k_{\perp} v_t} \left( \frac{z}{l} \right)^{1-\alpha}, \quad (75)$$

with the corresponding gain

$$G \sim [1 + \ln(t/t'_{\text{crit1}})] \frac{\Gamma I_0 k l}{\alpha k_{\perp} v_t} \left( \frac{z}{l} \right)^{1-\alpha} \quad \text{for } t > t'_{\text{crit1}}. \quad (76)$$

Here  $t'_{\text{crit1}} = (\Gamma I_0 k l / (\alpha k_{\perp} v_t^2)) (z/l)^{1-2\alpha}$ .

If the largest eddy sizes are of the order of the atmospheric scale height, and if velocities associated with those scales are of the order of the average wind velocity, the effect of turbulence (for all  $k_{\perp}$ ) will be comparable with the effect of systematic wind shear [the lower half of Eq. (71)]. Note that for this choice of  $v_t$  and  $l$ ,  $\epsilon_t \sim 2 \times 10^2 \text{ cm}^2 \text{ s}^{-3}$ . Measured values of  $\epsilon_t$  appear to be highly variable and generally in the  $10^{-1} - 10^3 \text{ cm}^2 \text{ s}^{-3}$  range.<sup>12</sup>

## VI. Summary and Discussion

Figures 2 and 3 are our main results. They locate the regions in the  $k_{\perp} - t$  (or equivalently  $k_{\perp} - \tau$ ) plane (at constant  $N_D$ ) in which different physical effects dominate. Figure 3 labels the regions by the physical effect, while Fig. 2 labels the regions by the instability growth (or decay) rates.

Note that there is no apparent advantage in putting all the energy into a single short pulse. Earlier work (e.g., Ref. 4) found that at large times the logarithmic gain of the perturbations grew as  $k_{\perp}^{2/3}$ , reached a constant value ( $\sim N_D^{1/2}$ ) for larger  $k_{\perp}$ , and then decayed exponentially from thermal diffusion above some critical  $k_{\perp}$ . It is apparent from Fig. 2 that for pulses of the same total energy, as the pulse time is lowered (for example, if  $N_D = 1000$  and  $t < 10^{-2} \text{ s}$ ), the gain at small  $k_{\perp}$  is lowered. This is true because the heating of the atmosphere does not instantaneously lower the density. A delay of the order of the sound crossing time of the perturbation occurs before isobaric conditions are reached. Thus the index of refraction does not change as much for short times as it does for long pulse times.

However, at large enough  $k_{\perp}$ , the sound crossing time of the perturbation is short enough, so that the density can be lowered to reach the maximum gain ( $\sim N_D^{1/2}$ ). Furthermore, at short times the diffusion cutoff occurs at even shorter length scales than at long times. Thus the spectral band in  $k_{\perp}$  over which the perturbations have grown large has become wider (in addition to shifting to larger  $k_{\perp}$ ). Since  $N_D$  can be quite large the optical quality of the beam can be highly degraded. [Of course, the exact amount of degradation depends on the amplitude of the initial noise spectrum  $I_1(k_{\perp}, t = 0)$ .]

In contrast, at large times, the effect of wind shear and turbulence begins to reduce the distortion. Figure 2 indicates that for  $N_D = 1000$  and for a pulse length of  $\sim 1 \text{ s}$ , wind shear and turbulence reduce the maximum gain from  $\exp(\sim 30)$  to  $\exp(\sim 3)$ . This is based on the assumption that the shearing gradient scale is an atmospheric scale height (5 km) and the change in wind velocity is  $\sim 450 \text{ cm s}^{-1}$  ( $\sim 10 \text{ mph}$ ), or that the turbulent velocity and associated turbulent cell scale size are given by the same respective parameters. Since both wind shear and turbulence can vary from site to site and as a function of time, experimental atmospheric data are required to evaluate an optimum pulse time more accurately.

In this paper we have concentrated on the case of a freely propagating beam; the short pulse effects for a phase-compensated beam are the subject of current research by the author. The main objective of this paper has been to obtain the basic scaling laws for the fine scale thermal-blooming instability. We should note, however, that we have treated the distortion number  $N_D$  as a known constant and the atmospheric velocity profile as given, both of which need better experimental determination. Furthermore, the growth rates we have obtained should be regarded as indicative; future numerical work will be required to

model accurately the complexity of the atmospheric density, velocity, and absorptivity profiles.

Finally, we should emphasize that Figs. 1 and 2 reflect the growth rates for single pulses with the same energy per pulse. A multipulse scheme to deliver the same energy will require a separate analysis, although the present work should lay much of the groundwork for such an exercise.

I wish to thank E. T. Scharlemann for suggesting this project and useful and encouraging discussions and also R. J. Briggs for his discussions as well, particularly his suggestion to use the WKB method for wind shear and his pointing out the importance of turbulent phase mixing. I would also like to thank R. J. Hawkins for critical reading of this manuscript and useful suggestions. This work was performed jointly under the auspices of the U.S. Department of Energy by Lawrence Livermore National Laboratory under contract W-7405-ENG-48 for the Strategic Defense Initiative Organization and the U.S. Army Strategic Defense Command in support of SDIO/SDC-ATC MIPR, W31RPDC-8-D5005.

#### References

1. D. C. Smith, "High-Power Laser Propagation: Thermal Blooming," *Proc. IEEE* 65, 1679 (1977).
2. J. R. Morris, "Unstable Growth of Perturbations in Thermal Blooming of Collimated Beams," presentation at SDIO Workshop, Kirkland AFB, NM, 15 Sept. 1987.
3. J. F. Schonfeld, "Time Dependent Thermal Blooming/Turbulence Propagation Code: Design, Motivations, Requirements," Lincoln Laboratory, Lexington, MA, BCP-3 (1987).
4. R. J. Briggs, *Models of High Spatial Frequency Thermal Blooming Instabilities*, Lawrence Livermore National Laboratory, Livermore, CA UCID-21118 (1987).
5. A. J. Glass, "A Possible Strategy for Compensation of the Thermal Rayleigh Instability," 4 Aug. 1987.
6. M. Rosenbluth, "Thermal Blooming in the Presence of Wind Shear," 3 Aug. 1987.
7. F. W. Perkins, "Filamentation Instabilities," 3 Aug. 1987.
8. T. J. Karr, *Thermal Blooming Compensation Instabilities*, Lawrence Livermore National Laboratory, Livermore, CA, UCID 21172 (1987).
9. K. A. Brueckner and S. Jorna, "Linearized Theory of Laser-Induced Instabilities in Liquids and Gases," *Phys. Rev.* 164, 182 (1967).
10. V. V. Vorobev and V. V. Shemetov, "Stability of a Light Beam and Its Decomposition with Thermal Self-Stress in a Moving Medium," *Izv. Vyssh. Uchebn. Zaved. Radiofiz.* 21, 1610 (1978) [*Sov. Phys.* 33, 1119 (1979)].
11. L. D. Landau and E. M. Lifshitz, *Fluid Mechanics* (Pergamon, London, 1959), Chap. 1 and 2.
12. N. K. Vinnichenko, N. Z. Pinus, S. M. Shmeter, and G. N. Shur, *Turbulence in the Free Atmosphere* (Consultants Bureau, New York, 1980).
13. L. D. Landau and E. M. Lifshitz, *Fluid Mechanics* (Pergamon, London, 1959), Chap. 3.
14. H. Tennekes and J. L. Lumley, *A First Course in Turbulence* (MIT Press, Cambridge, 1972).
15. M. M. Stanisic, *The Mathematical Theory of Turbulence* (Springer-Verlag, New York, 1985).
16. R. J. Briggs, (Lawrence Livermore National Laboratory); private communication.